

## SUPPORTING INFORMATION

### Antibody Controls

The specificity of the primary antibody against DGL $\alpha$  has previously been extensively characterized (Katona et al., 2006). Brain sections were incubated simultaneously with the antibody used in this study and with another antibody raised against a different epitope of the DGL $\alpha$  protein (termed L26 in Katona et al., 2006). The two antibodies revealed identical immunostaining patterns (Katona et al., 2006). More recently, brain sections obtained from DGL $\alpha$  knock-out mice (Tanimura et al., 2010) were immunostained for DGL $\alpha$  with the antibody used in this study. No immunostaining was observed in these sections (Ludányi et al., 2011).

The specificity of the primary antibody against NAPE-PLD has also been extensively tested earlier (Nyilas et al., 2008). Sections from the brain of NAPE-PLD knock-out mice (Leung et al., 2006) were negative for NAPE-PLD, whereas wild-type mice showed a characteristic immunostaining identical to that observed in rats (Nyilas et al., 2008).

Since the control experiments described earlier were performed in higher brain areas we have repeated these experiments in spinal cord samples. NAPE-PLD knockout mice were generated by Richard Palmiter and Serge Luquet (Liu et al., 2008). Briefly, a 4.4 kb EcoRI/NaeI fragment containing the exon 2 (left arm) of the *NAPE-PLD* and the 6.5 kb NaeI/NheI fragment (right arm) containing the exon 3 were subcloned in the 4517D plasmid to generate the targeting construct. LoxP sites were positioned to flank exon 3. The *Sv-Neo* (SV40 promoter-*neomycin-phosphotransferase*) gene was flanked by *frt* sites for removal by the action of FLPase. The targeting construct contained a *Pgk-diphtheria toxin A* gene at the 5' end of the left arm and an HSV *thymidine kinase* gene at the 3' end of the right arm for negative selection. Linearized plasmid (20  $\mu$ g) was electroporated into  $\sim 10^7$  AK18.1

embryonic stem cells (129S4/SvJaeSor; provided by P. Soriano) and plated on mitomycin C-treated SNL feeders and selected in G418 (300 µg/ml) and gancyclovir (2 µM). Individual colonies were picked, expanded for analysis, correctly targeted clones (5/80) were identified by Southern blot, and injected into blastocysts. After removal of the *Sv-Neo* cassette by breeding with FLP<sub>r</sub> mice, exon 3 was removed in all cells by breeding with *Mox2-Cre* mice (Tallquist and Soriano, 2000) to generate heterozygous animals with one null *NAPE-PLD* allele. These mice were bred with C57BL/6 mice to remove the *Mox2-Cre* gene, and then bred together to generate mice homozygous for the *NAPE-PLD*-null allele. Mice are on a mixed 129S4 x C57Bl/6 genetic background. Sections from the spinal cord of *NAPE-PLD* knock-out mice were negative for *NAPE-PLD*, whereas wild-type littermates showed a characteristic immunostaining identical to that observed in rats (Supporting Information Figure 1).

Unfortunately we were not able to obtain tissue samples from *DGLα* knock-out mice. For this reason, to control the specificity of our antibody against *DGLα* spinal cord sections were double-immunostained with the antibody used in this study (epitope: 790-908 aa; termed INT in Katona et al., 2006) and with another antibody raised against a different epitope of the *DGLα* protein (epitope: 1001-1042 aa) that we purchased from the Frontier Institute Co. (Ishikari, Hokkaido, Japan). The two antibodies revealed identical immunostaining patterns (Supporting Information Figure 2).

The specificity of the primary antibody against *DGLα* was also checked in a pre-adsorption test. The purified epitope of the *DGLα*-peptide (epitope: 790-908; in 1 µg/ml concentration) against which the primary antibody was raised was mixed with the antibody (diluted 1:1000), left at 4 °C for 16-18 hours and then centrifuged. Sections of the rat spinal cord were incubated according to the single immunostaining protocol by using the antibody against *DGLα* treated with the fragment of *DGLα*-peptide as primary serum. Under these

conditions, specific immunostaining was completely abolished (Supporting Information Figure 3).

To obtain a more global view about the specificity of the anti-DGL $\alpha$  and anti-NAPE-PLD antibodies a Western-blot analysis was performed on 3 rats. While the animals were deeply anesthetized with sodium pentobarbital (50 mg/kg, i.p.), the spinal dorsal horn at the level of L3-L5 lumbar segments were dissected. The dorsal horn was sonicated in 20 mM Tris lysis buffer (pH 7.4) containing the following protease inhibitors (mM): EDTA (4.0), EGTA (2.5), PMSF (0.002) benzamidine (0.013), pepstatine A (0.004), soybean trypsin inhibitor (0.001), leupeptine (0.001) and aprotinin (0.001). After removing cell debris from the sonicated samples with centrifugation (1500 g for 10 minutes at 4°C), the supernatant was centrifuged again (12,000 g for 20 minutes at 4°C). The pellet was re-suspended in lysis buffer containing 1% Triton X-100 and 0.1% SDS, and the samples were run on 10% SDS-polyacrylamide gels according to the method of Laemmli (1970). The separated proteins were electrophoretically transferred onto PVDF membranes (catalog no.: IPVH00010, Millipore, Billerica, MA, USA), and the membranes were immunostained according to the single immunostaining protocol described above. The immunostaining revealed only one immunoreactive band at molecular weight of 115 kDa for DGL $\alpha$  (Supporting Information Figure 4a) and 46 kDa for NAPE PLD (Supporting Information Figure 4b) corresponding to the molecular weight of the enzymes (Bisogno et al., 2003; Okamoto et al., 2004).

To test the specificity of the immunostaining protocol, free-floating sections were incubated according to the single immunostaining protocol described above with primary antibodies omitted or replaced with 1% normal goat serum. No immunostaining was observed in these sections.

**SUPPORTING INFORMATION****FIGURE LEGENDS**

**Supporting Information Figure 1:** Specificity of the anti-NAPE-PLD antibody.

Photomicrographs show immunoreactivity for NAPE-PLD in wild type (a) and knock out (b) mice. NAPE-PLD immunostaining can be observed in the dorsal horn of the wild-type mouse, while the immunoreactivity is completely absent from the dorsal horn of the NAPE-PLD knock out mouse. Scale bars: 100  $\mu$ m

**Supporting Information Figure 2:** Specificity of the anti- DGL $\alpha$  antibody. Micrographs of a single 1  $\mu$ m thick laser scanning confocal optical section which was double-immunostained with the antibody used in this study (INT; red; a) and with another antibody raised against a different epitope of the DGL $\alpha$  protein (FRONTIER; green; b). Mixed colors (yellow) on the superimposed image (c) indicate that the two antibodies revealed identical immunostaining patterns. Scale bar: 1  $\mu$ m

**Supporting Information Figure 3:** Specificity of the anti- DGL $\alpha$  antibody.

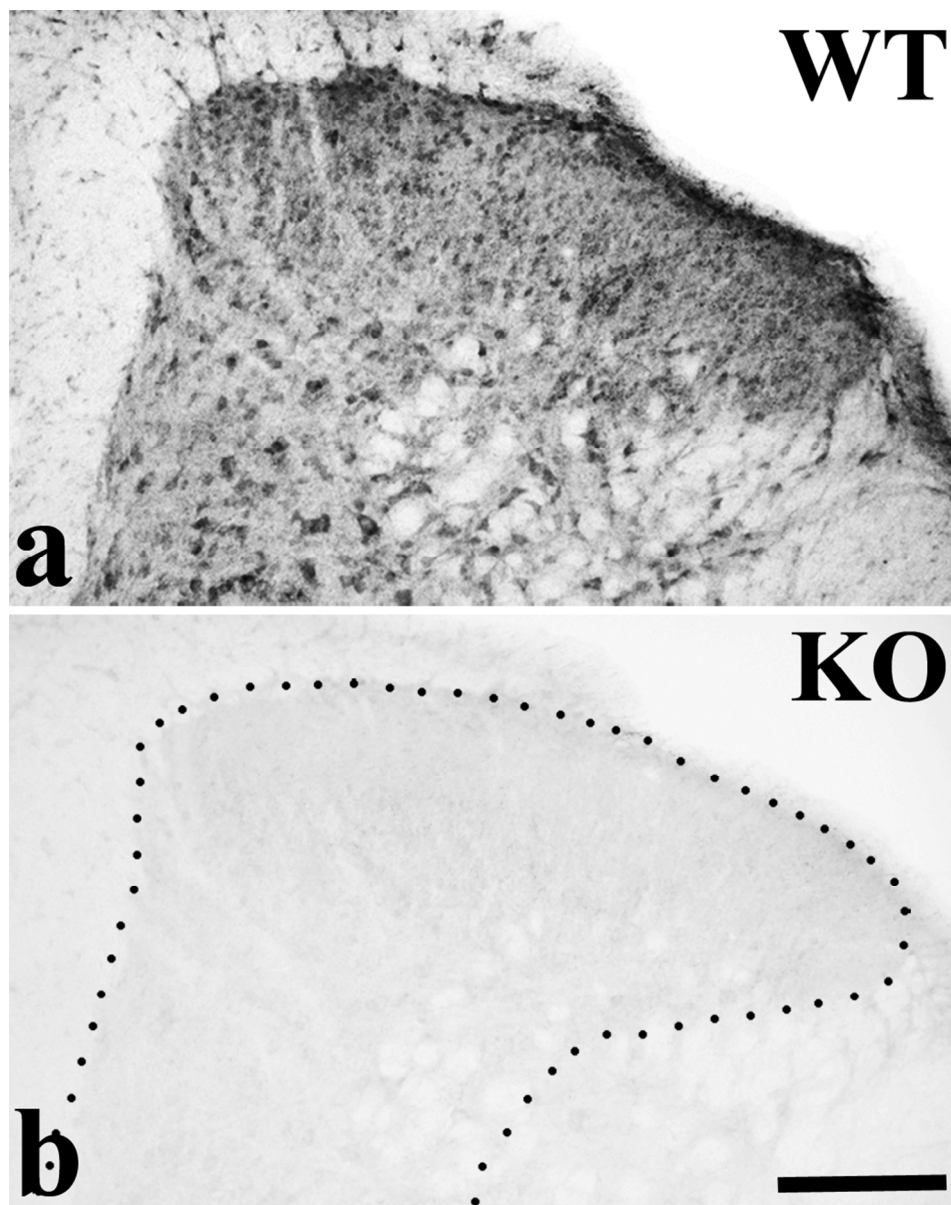
Photomicrographs of the spinal dorsal horn of rats showing (a) immunoreactivity for DGL $\alpha$ , and (b) the lack of specific immunostaining after the application of anti- DGL $\alpha$  antibody treated with the purified epitope of the DGL $\alpha$ -peptide (epitope: 790-908 aa) against which the primary antibody was raised. Scale bar: 100  $\mu$ m

**Supporting Information Figure 4:** Western blot analysis of the anti-DGL $\alpha$  and NAPE-PLD antibodies. The single immunoreactive bands on the Western blots indicate that the antibodies

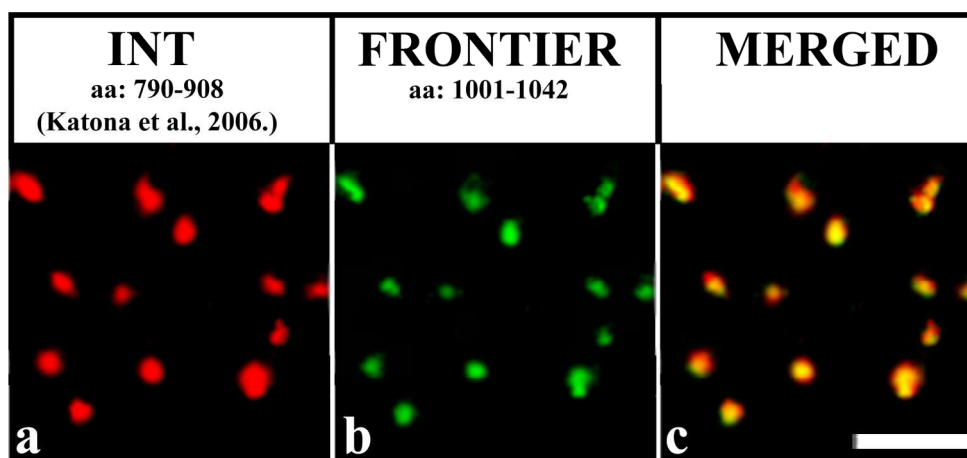
detect proteins with a molecular mass of ~115 kDa (a) and 46 kDa (b) that correspond to the molecular mass of DGL $\alpha$  (a) and NAPE-PLD (b) , respectively.

**Supporting Information Figure 5:** Co-localization of DGL $\alpha$  and NAPE-PLD with axonal and glial markers. Low power photomicrographs of sections double immunostained for DGL $\alpha$  (green; a, c, e, g, I, k) or NAPE-PLD (green; b, d, f, h, j, l) and markers that are specific for axon terminals of specific populations of peptidergic (CGRP, red; a, b) and non-peptidergic (IB4-binding, red; c, d) nociceptive primary afferents, axon terminals of putative excitatory (VGLUT2, red; e, f) and inhibitory (GAD65/67, red; g, h) intrinsic neurons, astrocytes (GFAP, red; i, f) and microglial cells (CD11b, red; k, l);. Note that because of the thickness of the confocal section (the thickness of confocal images acquired with an objective lense of 10x magnification is 10.4  $\mu$ m) mixed colors (yellow) do not necessarily indicate co-localization here. Scale bar: 200  $\mu$ m

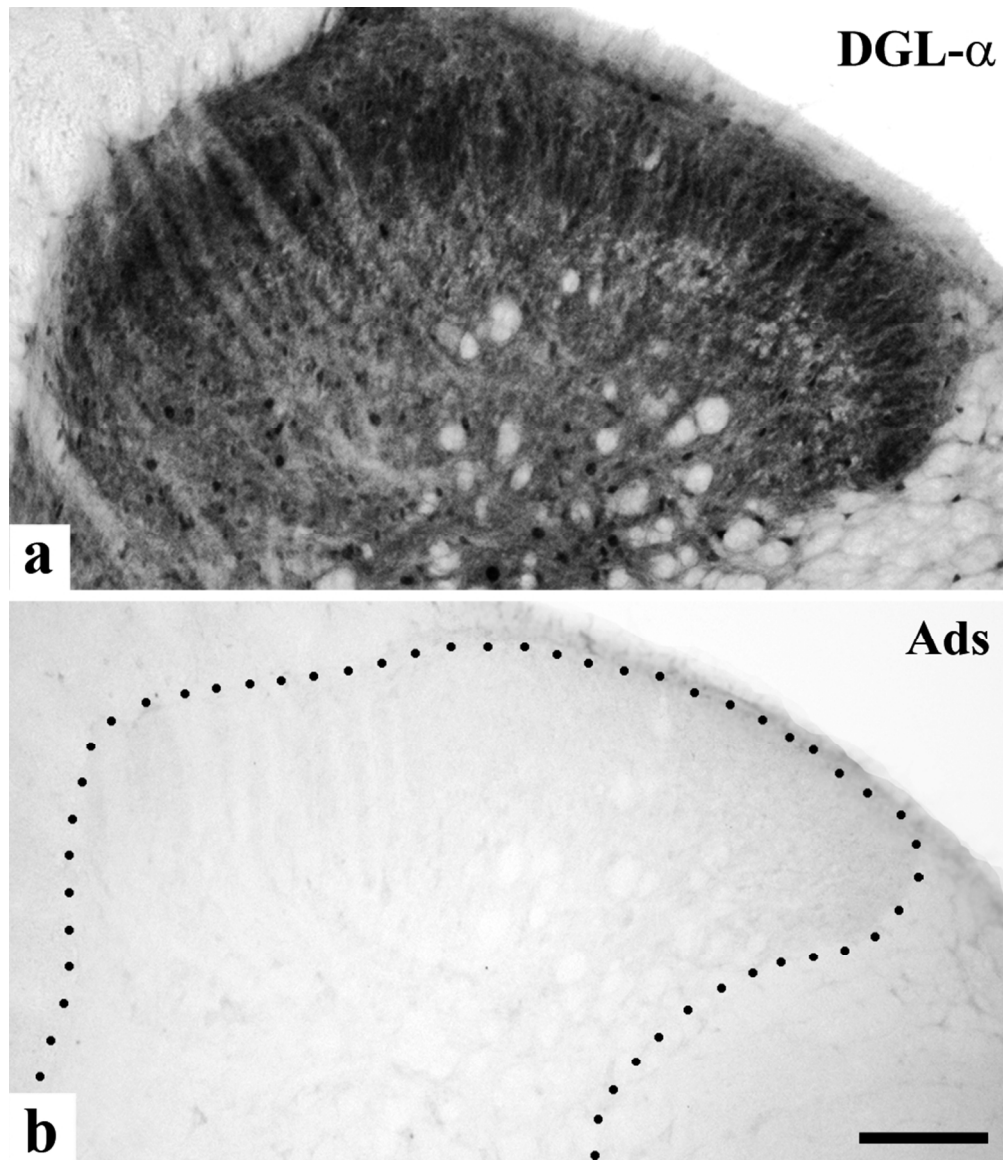
**Supporting Information Figure 6:** Lack of co-localization between IB4-binding and immunostaining for glial markers. Micrographs of single laser scanning confocal optical sections illustrating IB4-binding (red) and immunostaining of markers that are specific for astrocytes (GFAP, green; a, b) and microglial cells (CD11b, green; c, d) in the superficial spinal dorsal horn with low (a, c) and high (b, d) magnification. Note that mixed colors (yellow) that may indicate double labeled structures are not observed on the superimposed images obtained with high magnification. Scale bar: 200  $\mu$ m (a, c), 5  $\mu$ m (b, d)



Supporting Information Figure 1: Specificity of the anti-NAPE-PLD antibody. Photomicrographs show immunoreactivity for NAPE-PLD in wild type (a) and knock out (b) mice. NAPE-PLD immunostaining can be observed in the dorsal horn of the wild-type mouse, while the immunoreactivity is completely absent from the dorsal horn of the NAPE-PLD knock out mouse. Scale bars: 100  $\mu$ m  
87x110mm (300 x 300 DPI)

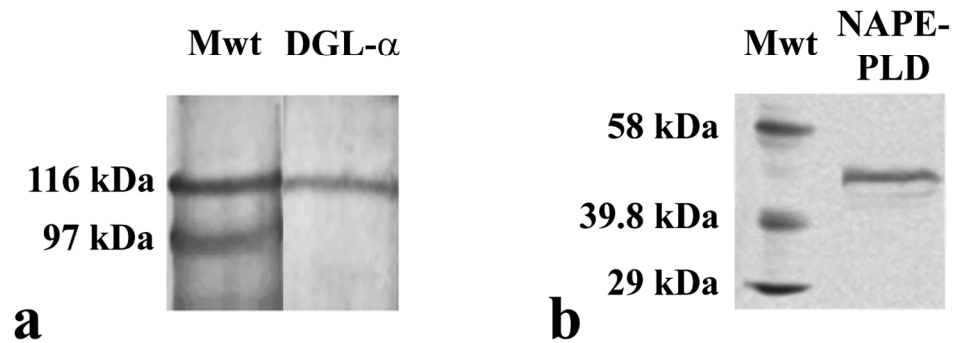


Supporting Information Figure 2: Specificity of the anti- DGLa antibody. Micrographs of a single 1 $\mu$ m thick laser scanning confocal optical section which was double-immunostained with the antibody used in this study (INT; red; a) and with another antibody raised against a different epitope of the DGLa protein (FRONTIER; green; b). Mixed colors (yellow) on the superimposed image (c) indicate that the two antibodies revealed identical immunostaining patterns. Scale bar: 1  $\mu$ m  
180x87mm (300 x 300 DPI)

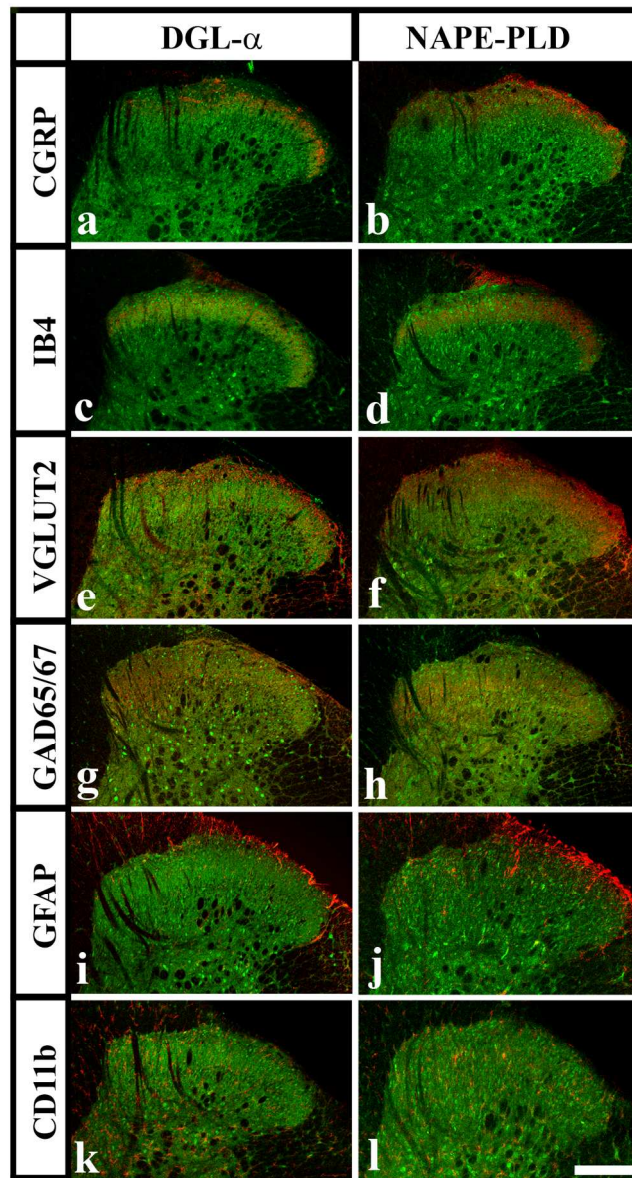


Supporting Information Figure 3: Specificity of the anti- DGL $\alpha$  antibody. Photomicrographs of the spinal dorsal horn of rats showing (a) immunoreactivity for DGL $\alpha$ , and (b) the lack of specific immunostaining after the application of anti- DGL $\alpha$  antibody treated with the purified epitope of the DGL $\alpha$ -peptide (epitope: 790-908 aa) against which the primary antibody was raised. Scale bar: 100  $\mu$ m  
87x101mm (300 x 300 DPI)

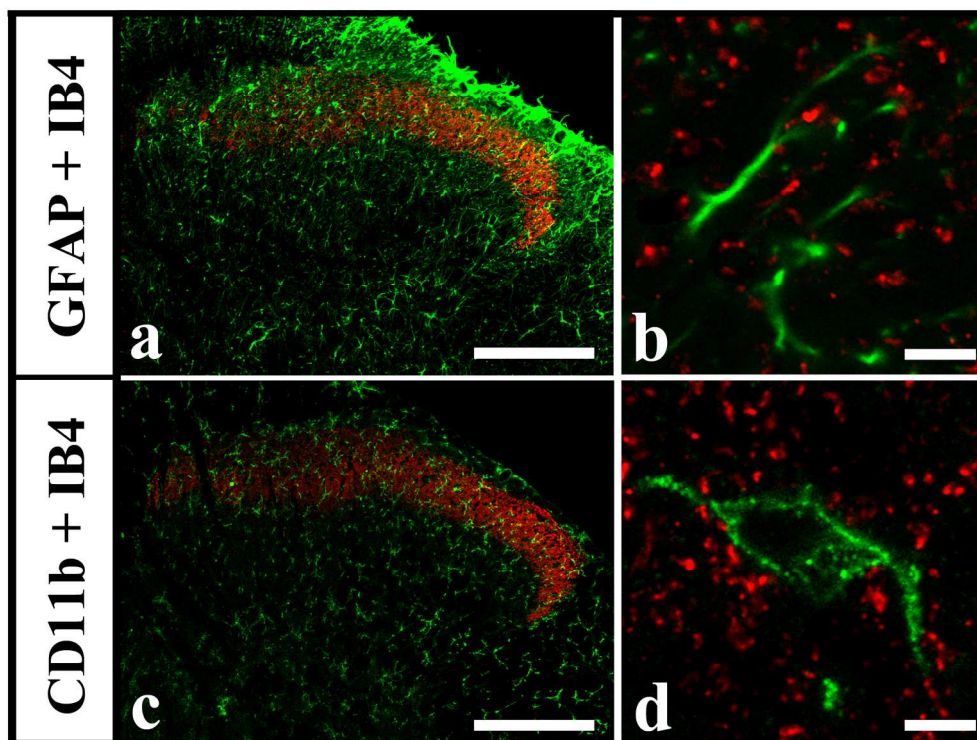




Supporting Information Figure 4: Western blot analysis of the anti-DGL $\alpha$  and NAPE-PLD antibodies. The single immunoreactive bands on the Western blots indicate that the antibodies detect proteins with a molecular mass of  $\sim$ 115 kDa (a) and 46 kDa (b) that correspond to the molecular mass of DGL $\alpha$  (a) and NAPE-PLD (b), respectively.  
129x51mm (300 x 300 DPI)



Supporting Information Figure 5: Co-localization of DGL $\alpha$  and NAPE-PLD with axonal and glial markers. Low power photomicrographs of sections double immunostained for DGL $\alpha$  (green; a, c, e, g, I, k) or NAPE-PLD (green; b, d, f, h, j, l) and markers that are specific for axon terminals of specific populations of peptidergic (CGRP, red; a, b) and non-peptidergic (IB4-binding, red; c, d) nociceptive primary afferents, axon terminals of putative excitatory (VGLUT2, red; e, f) and inhibitory (GAD65/67, red; g, h) intrinsic neurons, astrocytes (GFAP, red; i, f) and microglial cells (CD11b, red; k, l);. Note that because of the thickness of the confocal section (the thickness of confocal images acquired with an objective lens of 10x magnification is 10.4  $\mu$ m) mixed colors (yellow) do not necessarily indicate co-localization here. Scale bar: 200  $\mu$ m  
109x199mm (300 x 300 DPI)



Supporting Information Figure 6: Lack of co-localization between IB4-binding and immunostaining for glial markers. Micrographs of single laser scanning confocal optical sections illustrating IB4-binding (red) and immunostaining of markers that are specific for astrocytes (GFAP, green; a, b) and microglial cells (CD11b, green; c, d) in the superficial spinal dorsal horn with low (a, c) and high (b, d) magnification. Note that mixed colors (yellow) that may indicate double labeled structures are not observed on the superimposed images obtained with high magnification. Scale bar: 200  $\mu\text{m}$  (a, c), 5  $\mu\text{m}$  (b, d)  
180x136mm (300 x 300 DPI)